

ORIGINAL RESEARCH

Spectral pattern study of citrus black rot caused by *Alternaria alternata* and selecting optimal wavelengths for decay detection

Narges Ghanei Ghooshkhaneh¹  | Mahmood Reza Golzarian¹  | Mojtaba Mamarabadi²

¹Department of Biosystems Engineering, Ferdowsi University of Mashhad, Mashhad, Iran

²Department of Plant Protection, Ferdowsi University of Mashhad, Mashhad, Iran

Correspondence

Mahmood Reza Golzarian, Department of Biosystems Engineering, Ferdowsi University of Mashhad, 1163, Mashhad, Iran.

Email: m.golzarian@um.ac.ir

Funding information

This work was supported by Ferdowsi University of Mashhad [grant numbers 3/48638]; the Iran National Science Foundation: INSF [grant number 98000184].

Abstract

Fungal decay is one of the most common diseases that affect postharvest operations and sales of citrus. Sometimes, fungal disease develops and spreads inside the fruit and in the advanced stages of the disease, it appears apparent, so the use of efficient and reliable methods for early detection of the disease is very important. In this study, early detection of citrus black rot disease caused by *Alternaria* genus fungus was examined using spectroscopy. Jaffa oranges were inoculated with *Alternaria alternata*. The samples were inspected by spectroscopy (200–1100 nm) in the 1st, 2nd, and 3rd weeks after inoculation. The classification of healthy and infected samples and selection of most important wavelengths were conducted by soft independent modeling of class analogy (SIMCA). The most important wavelengths in the detection of healthy and infected samples of the 1st week were 507, 933, 937, and 950 nm with a classification accuracy of 60%. The most important wavelengths of the 2nd week were 522 and 787 nm with a classification accuracy of 60%. Also, wavelengths of 546, 660, 691, and 839 were found to be effective in the 3rd week with a classification accuracy of 100%.

KEYWORDS

fast detection, fungi infection, postharvest decay, spectral analysis, spectroscopy

1 | INTRODUCTION

Citrus is considered the most cultivated fruit in the world and the annual production of more than 80 million tons shows its importance in the world economy (Moltó et al., 2010). Postharvest defects of citrus may be morphological, physical, and physiological disorders or pathological (Guleria, 2000). Pathogenic fungi cause postharvest losses in citrus fruits in the packaging, transportation, and storage process (Timmer et al., 2003). Citrus black rot is a significant postharvest problem caused by *Alternaria alternata* (El-Otmani

et al., 2011). Fungal spores may be latent on the citrus calyx and invade the columella when the fruit ripens. Then, it spreads easily along the columella (Peever et al., 2005). The rot spreads slowly and the disease is not controlled by pre- and postharvest fungicides (Timmer et al., 2003). It affects mainly navel oranges, but it can infect all citrus fruits when appropriate condition is prepared (Mojerlou, 2012).

Infected fruits ripen well before maturity and some of them fall off before harvest. The optimum conditions for *Alternaria* infections are temperatures from 23 to 27°C, but still, it can grow

This is an open access article under the terms of the [Creative Commons Attribution](https://creativecommons.org/licenses/by/4.0/) License, which permits use, distribution and reproduction in any medium, provided the original work is properly cited.

© 2022 The Authors. *Food Science & Nutrition* published by Wiley Periodicals LLC

at temperatures between 0 and 10°C, so with a temperature of 21°C, the disease develops after 5 weeks, and in cold warehouses, the symptoms of the disease become observable up to 10 weeks (Troncoso-Rojas & Tiznado-Hernández, 2014). Disease Symptoms begin as light brown spots from the end of the fruit and gradually develop on the surface of the fruit opposite the calyx. Due to the production of ethylene in response to infection, the fruit loses its green color and the surface spots turn dark brown (Timmer, et al., 2003). As a result, early detection of this infection, which is in the form of core rot without any external symptoms of infection, has great importance in the stages before, during, and after storage in the warehouse. In addition, *Alternaria alternata* produces different kinds of toxic metabolites that have potential hurts to human health (Gabriel et al., 2017). Hence, separation of infected fruits is also critical for the juice industry.

In recent years, due to the increasing awareness of consumers of agricultural products, many advances have been made in the development of nondestructive techniques for determining the internal quality and safety of products. Recently, optical sensing technology has become available as a potential tool for nondestructive analysis and assessment of the quality and safety of agricultural products. Spectroscopy is a promising way to determine essential food qualities by measuring optical properties (Bock & Connelly, 2008), which, over the past two decades, has been rapidly developed to examine the internal quality factors of agricultural products (Zude, 2009). Factors such as generality in the world, broad usability, simple and inexpensive equipment and implementation, and time saving in attaining results are outstanding advantages of this method in terms of quantitative and qualitative analysis (Beć & Huck, 2019). It also does not require the use of chemical reagents, and measures many parameters in a single analysis (García-Sánchez et al., 2017). Compared to microbiological methods used to detect biological organisms such as fungi and bacteria that are very time consuming, tedious, and expensive, spectroscopy is cheaper and faster (Alander et al., 2013).

Researchers frequently used spectroscopy to predict internal properties including the soluble solids content (SSC) and firmness of apple (Bobelyn et al., 2010); total soluble solids and titratable acidity of mandarin (Antonucci et al., 2011); vitamin c, total polyphenol, and sugar content of apple (Pissard et al., 2013); maturity index of mango (Jha et al., 2014); total soluble solids content, pH, titratable acidity, ascorbic acid content, and phenolic content of strawberry (Amodio et al., 2017); flesh firmness of peach (Uwadaira et al., 2018); the maturity of watermelon (Jie et al., 2019); and moisture and soluble solids content of pear fruit (Mishra et al., 2021). In addition to predicting internal quality, extensive studies have been conducted for predicting the external quality of fruits with spectroscopy. In addition to the internal properties of total soluble solids and titratable acidity of Valencia oranges, color index and mass were also predicted by Fourier transform near-infrared reflectance (FT-NIR) spectroscopy (Magwaza et al., 2013). Moreover, the Fourier transform spectroscopy method was used to evaluate the color, soluble solids content, and physical parameters of apricot (Buyukcan & Kavdir, 2017). Weight, length, equatorial diameter, and color of

summer squash were determined by using near-infrared reflectance spectroscopy (Sánchez et al., 2018).

External characterizations of color, firmness, and pericarp wall thickness as well as internal quality like Brix, pH, malic acid, total phenolic compounds, ascorbic acid, and total carotenoid content were estimated (Toledo-Martin et al., 2015). Several external defects including storage disorders of kiwifruit (Clark et al., 2004); hardening pericarp disorder in intact mangosteen (Teerachaichayut et al., 2011); various potato surface defects, that is, mechanical damage, greening, common scab, and soil deposits on the skin (Riza et al., 2017); and rind pitting disorder of “marsh” grapefruit (Ncama et al., 2018) were evaluated with the NIR spectroscopy method. Furthermore, spectroscopic methods had been used for nondestructive internal quality assessment of brown core in the Chinese pear “yali” (Han et al., 2006), translucent flesh disorder in intact mangosteen (Teerachaichayut et al., 2007), *Bactrocera oleae* infestation of olive fruit (Moschetti et al., 2015), internal rot in onion bulbs (Kuroki et al., 2017), and internal browning in “Cripps pink” apples (Mogollon et al., 2019). Due to the fact that spectroscopy had been an effective method in detection of the internal defects, in this study, the detection of internal infection of oranges caused by *Alternaria alternata* with spectroscopy and selection of optimal wavelengths were studied.

2 | MATERIALS AND METHODS

2.1 | Orange inoculation with fungal pathogen suspension

Alternaria alternata isolated from infected oranges with black rot disease was grown in PDA medium and incubated at 25°C for 7 days. After spore germination, spore suspension was prepared. Thus, under a laminar hood, about 10 ml distilled sterile water was poured in the plate and scrapped gently with a sterile scalpel to release the spores. Then, a uniform suspension was prepared with a vortex mixer. For better dispersion of spores in distilled water, 0.5% of Tween 20 was added to spore suspension. At the end, spore density was determined using a hemocytometer and adjusted to 10⁶ spores/ml.

Jaffa oranges were purchased from Mashhad markets and transferred to the Plant Pathology Laboratory of Department of Plant Protection of Ferdowsi University of Mashhad. Oranges were used for spectral acquisition, including 45 oranges contaminated with *Alternaria* spores, and 30 healthy oranges. Healthy, similar size and ripen oranges (10.6 TSS and 2.58 pH at 21°C) were selected and washed. Sterilization was performed for 30 s in separate solutions of 2% hypochlorite, sterile distilled water, and 70% ethanol, respectively. Under sterile conditions, 0.02 ml of spore suspension with a concentration of 10⁶ spores/ml was injected into the middle part of the central axis of each orange. Sterile distilled water was also injected into the healthy samples. The samples were then placed in containers covered with plastic and incubated at 25°C.

2.2 | Spectral measurement

In order to investigate whether the structure of the fungus affects the spectral pattern of the product, an experiment was first performed with infected orange juice and healthy orange juice. According to the Iran National Standard of Soft Drinks – Fruit Juice and Fruit Juice Products – Microbiological Specification and Test Methods No. 3414, the maximum allowable mold in 1 ml is considered negative and the test method should be performed according to Standard No. 997 of mold and yeast test. In this standard, the test sample is added to the plate of the selected culture medium and the plates are incubated at 25°C for 3–5 days and the (colony) colonies of mold and yeast are examined and counted and their number in 1 g or 1 ml of the sample is reported. In the explained test, the exact concentration of fungus in fruit juice cannot be measured and it only shows the existence of fungal microorganisms in the suspension.

Spore suspension with a concentration of 10^6 spores/ml of *A. alternata* was prepared according to the concentration selected by Peña et al. (Peña et al., 2009). The orange juice was passed through a filter paper and diluted 1:9 with distilled water (1 part orange juice and 9 parts water). Since according to Beer Lambert's law, the concentration of the sample is effective in the spectroscopy of solutions, the high concentration of the sample increases the noise in the spectral response of the sample. For this reason, the solution is diluted, which was obtained by trial and error. An ultraviolet-Vis spectrophotometer (model: Biochrom WPA Biowave II) was used to measure the absorption of solutions. First, the spectrophotometer was calibrated with distilled water, and then the absorption value was measured for orange juice. Because the measured absorption value was more than 2.5, the spectrophotometer was calibrated with orange juice and the absorption value of infected orange juice was obtained in the range of 400–1100 nm at intervals of 100 nm. Also, an Ultraviolet -VIS spectrophotometer (model: Dynamica Halo XB-10 Ultraviolet-VIS Single Beam) was used for the acquisition of the continuous spectrum from orange juices in the range of 200–700 nm. To study the ability to detect the internal fungal infection, oranges were inoculated in laboratory conditions and a multichannel spectrometer (Model: Ava Spec-2048TEC-USB2-2) with Avasoft 7.5 2009 software was used to obtain the spectral curves of healthy and infected oranges for 3 consecutive weeks after inoculation. The spectral data were acquired in the range 200–1100 nm with a wavelength resolution of 1 nm. A 50 W tungsten/halogen lamp was used as the lighting source and interactance mode was used for spectral acquisition along the central axis of the fruit. In this mode, that is, an aggregation of transmission and reflection, illumination is applied by a fiber-optic cable in close touch with the sample. Light scatters inside the sample and three modes of reflection, transmission, and absorption occur with the internal components. The scattered light internal the sample returns to the detector through the same fiber-optic cable that is the illumination source. Surface reflection decreases due to the close touch between the fiber-optic and sample, and depth of penetration increases. Two modes of interactance and transmission can be used to gain information from deeper internal

TABLE 1 Spectroscopy results of fungal-infected orange juice

Wavelength (nm)	Absorption
400	0.735
500	0.625
600	0.498
700	0.380
800	0.352
900	0.260
1000	0.316
1100	0.505

parts of the sample. Since the detectors used are usually of the silicon type, they allow acquisition of spectral information in the range of 700–1100 nm. In this case, the measured properties can be moisture, sugar content, and even defects or internal disorders of agricultural products (Alander et al., 2013). The sample was inside a chamber that prevented ambient light from entering. The probe that was in contact with the sample transferred the light and received the transmitted light from the sample simultaneously. In order to obtain the relative spectrum, dark and white reference spectra were taken before each sample measurement. Then, according to Equation (1), the relative spectrum was calculated.

$$R = \frac{S - D}{W - D} \quad (1)$$

where R is the relative spectrum, S is the measured spectrum of each sample, D is the dark spectrum, and W is the white spectrum of the Teflon reference surface.

3 | RESULTS AND DISCUSSION

3.1 | Spectral pattern of healthy and infected orange juice

Table 1 shows the result of spectroscopy of fungal-infected orange juice in the range of 400–1100 nm with a 100 nm wavelength resolution. According to the results of Table 1, which are absorption values of infected orange juice proportional to healthy orange juice, it could be concluded that contamination of orange juice with spores of *Alternaria* fungus had an effect on its absorption and fungal-contaminated orange juice had a higher absorption value than healthy orange juice. The absorption decreased with increasing wavelength, and this decreasing trend existed up to 900 nm, and then increased again, which could be due to water absorption that occurs in the range of 980–1060 nm. Wavelengths in the region of 751–915 nm appear to be less affected by absorption of internal fruit components and, therefore, can include information about the scattered light through fruit tissue (Qing et al., 2007).

The absorption spectrum of three different samples of orange juice and infected orange juice is shown in Figure 1. As shown in

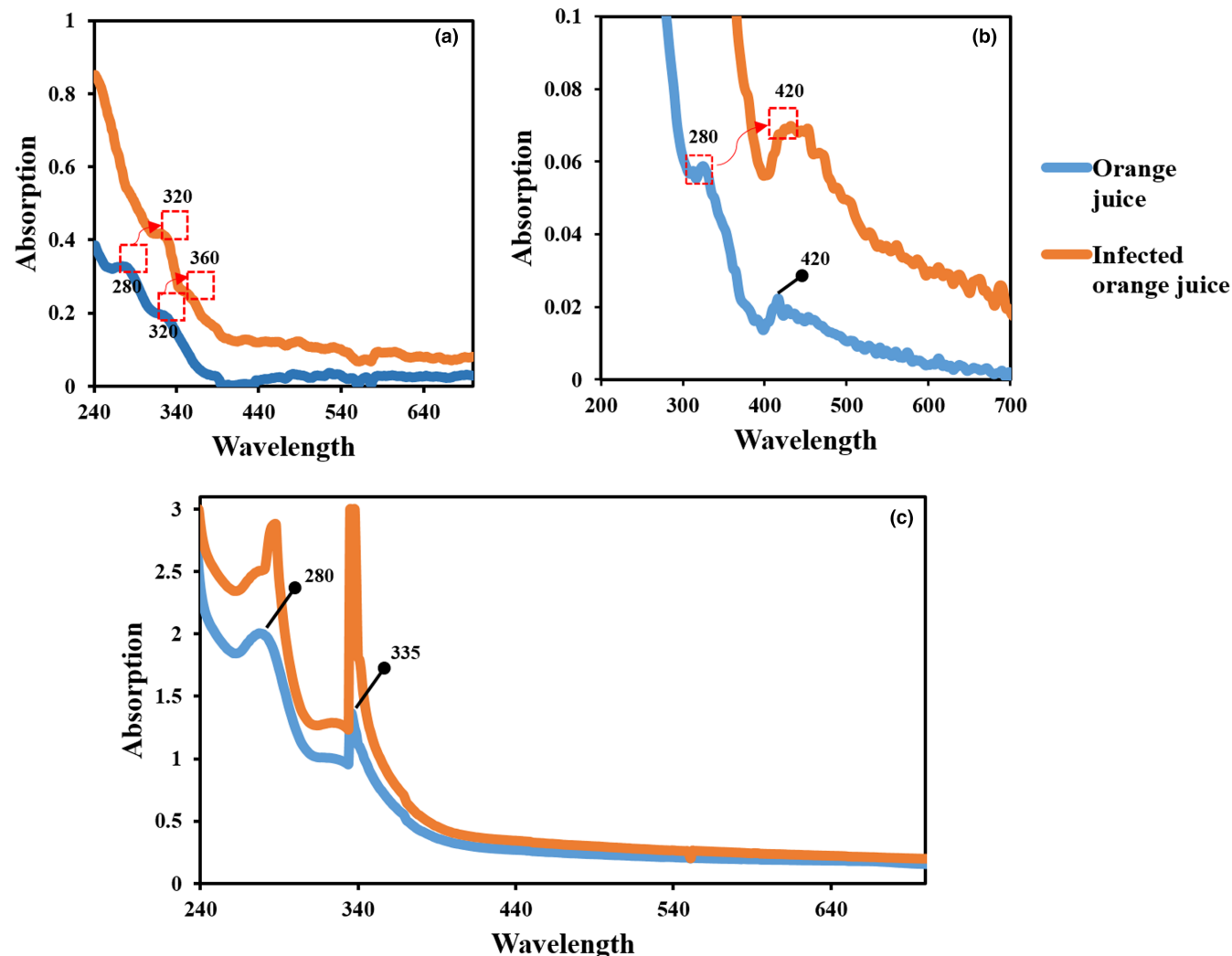


FIGURE 1 Absorption spectrum of orange juice and infected orange juice: (a) Sample No. 1, (b) Sample No. 2, and (c) Sample No. 3

Figure 1, samples of fungal-contaminated orange juice had a higher absorption than healthy orange juice samples. There are also some differences between healthy and contaminated orange juice due to the peaks. According to Figure 1a, there were two distinct spectral peaks around 280 and 320 nm for the orange juice sample. While in the curve of infected orange juice, two peaks around 320 nm and 360 nm could be identified. It can be said that adding fungus spores to orange juice had caused a peak shift from 280 nm to 320 nm and a peak shift from 320 nm to 360 nm. According to Figure 1b, there were two perceptible spectral peaks around 320 and 420 nm for the orange juice sample. However, there was only one peak in the curve of infected orange juice around 420 nm. Adding fungus spores to orange juice had caused a peak shift from orange juice peaks to 420 nm. As shown in Figure 1c, two peaks around 280 nm and 335 nm were distinguished in the orange juice curve but there was no peak shift, only a significant increase in the absorption of these wavelengths.

The major components of citrus juice which significantly affect the spectral absorption include carotenoids, flavonoids, polyphenols,

and ascorbic acid. The carotenoid pigments in citrus fruits and juice have very complicated chemistry. Wavelengths 425, 444, and 465 nm are related to carotenoids content, 325 nm to polyphenols, 280 nm to flavonoids, and 245 nm to ascorbic acid content (Cohen & Saguy, 1988). As a result, the peak around 280 nm in Figure 1a,b could be due to the presence of flavonoids, the peak around 320 and 335 nm in Figure 1a,c could be due to the presence of polyphenols, and the peak around 420 nm could be due to the presence of carotenoids in the orange juice.

The reason for the peak shift in fungal-infected orange juice curves could be related to the structure of the fungus spores or the sensitivity of this fungus to the ultraviolet region. The use of near-ultraviolet lamps (300–400 nm) increases the production of *Alternaria* fungus conidia (Carvalho et al., 2008). *Alternaria alternata* also caused blue fluorescence in tobacco leaves, which is mainly due to the accumulation of scopoletin due to pathogen attack. Scopoletin was considered as a significant phytoalexin that acts in contrast to microbial pathogens. “Phytoalexins are antimicrobial substances of low molecular weight produced by plants in response to pathogen

attack" (Sun et al., 2014). One of the coumarins present in fruits is scopoletin and its ultraviolet bands absorption are 252 and 344 nm (Abad-Garcia et al., 2009).

Scopoletin in young citrus fruits had a maximum excitation wavelength of 350 nm and maximum fluorescence of 460 nm (Goldschmidt et al., 1971). It can be concluded that one of the reasons for the formation of peaks and peak shifts in curves of fungal-infected orange juice was the increase in the amount of scopoletin in orange juice against the fungus attack.

3.2 | Spectral pattern of healthy and infected orange fruits

Each week spectroscopy was done on 15 samples and then the samples were cut to check the severity of the infection. Figure 2 shows the growth of infection in oranges after different incubation times. As shown, the decay area caused by fungal sporulation was a dark area inside the orange that was limited to the columella and juice sacs nearby to it, although it did not affect the peel. As confirmed in Figure 2, rotten areas were becoming larger over the time after inoculation. The infected area was restricted to the short part of injection in oranges incubated for 1 week after inoculation (Figure 2a), 2 weeks after inoculation almost half of the central axis was observed to be rotted (Figure 2b), and after 3 weeks, whole central axis and its nearby juice sacs were apparently decayed by *A. alternata* (Figure 2c).

Oranges were ranked by severity level from 0 to 3, where level 0 indicated no rotten area, level 1 indicated 1–2 cm² of the rotten area in the central axis, level 2 indicated that almost half the central axis rotted, and level 3 when whole of the central axis decayed by *A. alternata* (Peever et al., 2005). As explained, in this study, the rate of infection in the 1st week is on a scale of 1, in the 2nd week on a scale of 2, and in the 3rd week on a scale of 3.

Figure 3 shows the average interactance spectra of infected samples at different incubation times after inoculation. According to Figure 3, it can be concluded that as the infection spread in the

fruit, spectral backscattering decreased and in fact, the absorption rate increased. The average spectrum curve of the 1st week after inoculation had the highest reflectance, and spectral reflectance had decreased over time since inoculation.

"The key taxonomic feature of the genus *Alternaria* is the production of large, multicellular, dark-colored (melanized) conidia. The melanin that is present in the conidia is concentrated in the outer region of the primary cell walls, which are derived from the original wall of the developing spore, and in the septa, which delimit individual spore cells in the multicellular conidium." All organisms including animals, plants, and microorganisms generate dark color melanin pigments that have high molecular weight. They are created by the oxidative polymerization of phenolic or indolic compounds. Since polymerization does not pursue a precise schema, melanins have different structures of molecules with aromatic rings and hydroxyl groups. Melanin contains stable populations of free radicals (Thomma, 2003). Production of melanin pigments by *alternaria* can increase absorption in the NIR region (Pombeiro-Sponchiado et al., 2017).

Figure 4 shows the average interactance spectra of healthy and infected samples in the 1st week after inoculation. The wavelength region 550–700 nm represented the most variations in spectral curves between healthy and infected samples. Spectral peaks at 700 and 840 nm were observed.

Table 2 shows the results of comparing healthy and infected samples in the 1st week in different spectral ranges using paired *t*-test at the level of 5% error probability. The results of Table 2 show that there was a significant difference at the 5% level between healthy and infected samples in the 1st week after inoculation.

Figure 5 shows the first derivative curve of the average interactance spectrum in the 1st week after inoculation. According to the curve, the wavelength region of 500–700 nm represented the most variations in spectral curves between healthy and infected classes, suggesting that the important wavelengths for the distinction of two groups may belong to this region. In spite of the overlap in the range of 500–600 nm in the spectral curve in Figure 4, the first derivative curve of healthy and infected groups is significantly distinguishable from each other in the same range (spectral peak around 522 nm). In



FIGURE 2 Fungal growth in orange through 3 weeks after inoculation, (a) 1st week, (b) 2nd week, and (c) 3rd week after injection of the fungal suspension

FIGURE 3 Average interactance spectra of infected samples in the 1st, 2nd, and 3rd week after inoculation

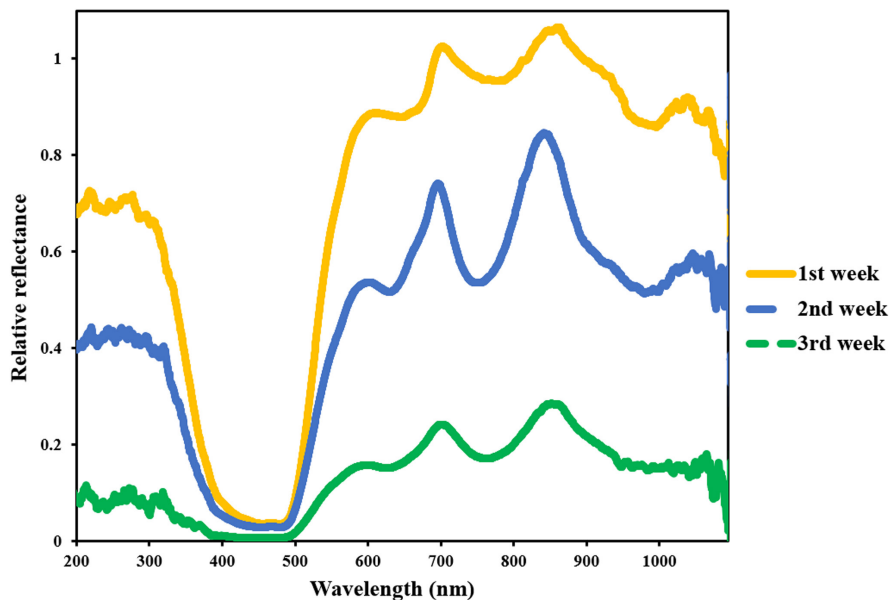


FIGURE 4 Average interactance spectra of healthy and infected samples in the 1st week after inoculation

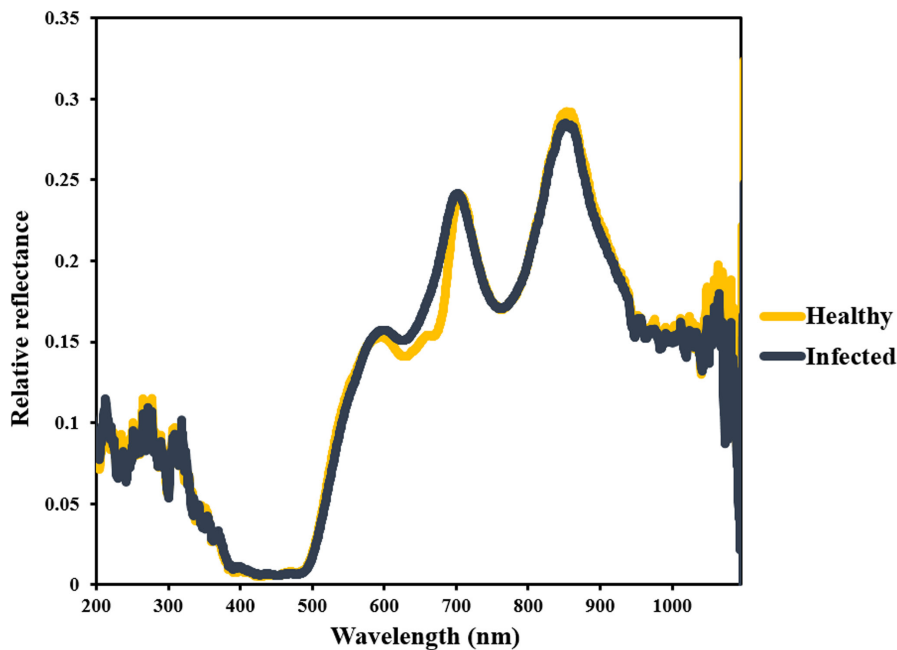


TABLE 2 Paired samples t-test to compare the spectral mean of healthy and infected orange samples in the 1st week after inoculation

Spectral range	Groups	Descriptive statistics		Results		
		Number	Mean	t	df	Sig (2-tailed)
200–1100 nm	Healthy	1627	0.1322	4.534	1626	0.000
	Infected	1627	0.1308			
550–700 nm	Healthy	263	0.0229	-14.658	263	0.000
	Infected	263	0.0307			

the range of 600–700 nm, the two wavelengths of 665 and 690 nm caused obvious differences between healthy and infected samples. Furthermore, in spite of the overlap between the healthy and infected classes in the range 700–800 nm of the raw curve, the healthy oranges

made a noticeable difference at the wavelength around 717 nm, proposing that it can be an effective wavelength for the distinction between two groups. At wavelengths of 941 and 950 nm, a higher peak was observed for fungal-infected samples than healthy samples.

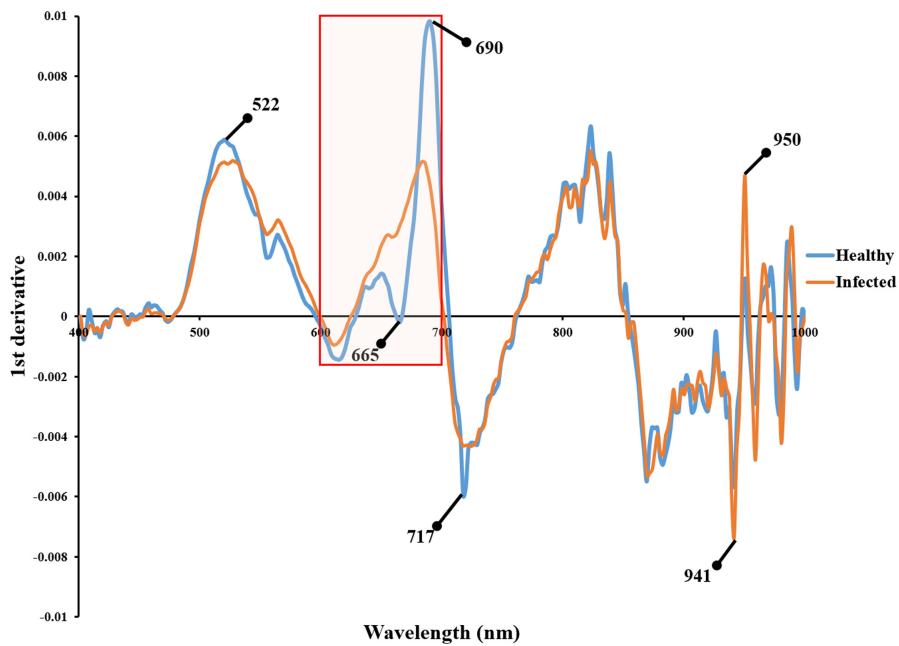


FIGURE 5 First derivative curve of average interactance spectrum in the 1st week after inoculation

Spectral range	Groups	Descriptive statistics		Results		
		Number	Mean	t	df	Sig (two-tailed)
400–1000 nm	Healthy	266	0.000543	0.205	265	0.838
	Infected	266	0.000528			
500–700 nm	Healthy	88	0.002772	-0.290	87	0.772
	Infected	88	0.001884			
600–700 nm	Healthy	45	0.003311	0.132	44	0.895
	Infected	45	0.001940			

TABLE 3 Paired samples *t*-test to compare the first derivative spectrum of healthy and infected orange samples in the 1st week after inoculation

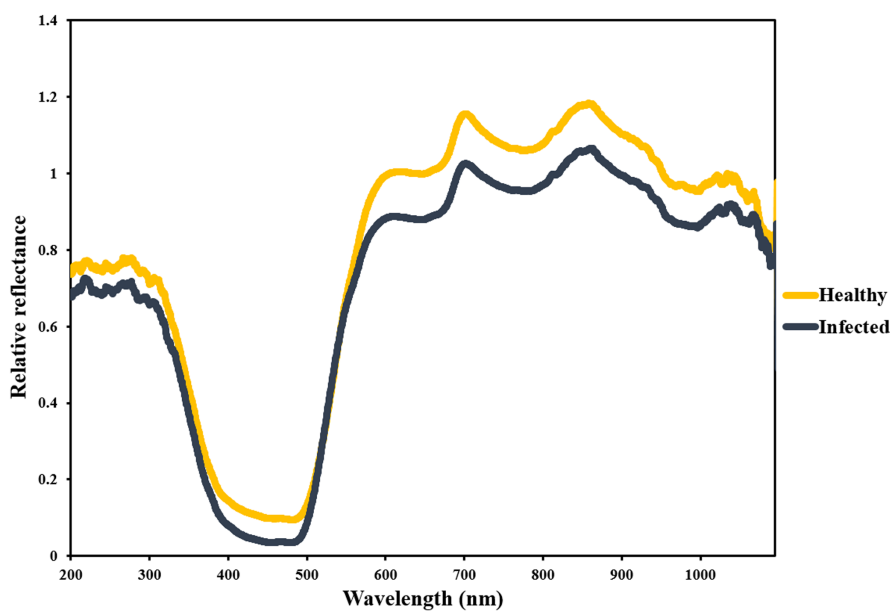


FIGURE 6 Average interactance spectra of healthy and infected samples in the 2nd week after inoculation

Table 3 shows the results of comparing the first derivative spectrum of healthy and infected samples in the 1st week in different spectral ranges using paired *t*-test at the level of 5% error probability. The results of Table 3 show that there was no significant difference between the first derivative spectrum of healthy and infected samples in the 1st week in different spectral ranges 400–1000 nm, 500–600 nm, and 600–700 nm. Thus, the first derivative spectrum was not used to select the optimal wavebands.

Figure 6 shows the average interactance spectra of healthy and infected samples in the 2nd week after inoculation. As shown in Figure 6, spectral curves of the two groups had an obvious difference in the spectral range of 550–1050 nm, and two peaks of 700 and 840 nm were observed same as in Figure 4.

Table 4 illustrates the results of comparing healthy and infected samples in the 2nd week in different spectral ranges using paired *t*-test at the level of 5% error probability. There was a significant difference at the 5% level between healthy and infected samples in the 2nd week after inoculation according to the results of Table 4.

As depicted in Figure 7, the mean spectra of the two groups were differentiated clearly on the entire spectral range and were distinguishable from each other.

The results of comparing healthy and infected samples in the 3rd week using paired *t*-test at the level of 5% error probability are illustrated in Table 5. It could be concluded from Table 5 that there was a significant difference at the 5% level between healthy and infected samples in the 3rd week after inoculation.

According to the curves and results of paired *t*-test, it can be concluded that healthy samples are separable from infected samples by spectral information and, for optimal separation of two classes, effective wavebands should be extracted. To find the effective wavebands, the soft independent modeling of class analogy was used.

3.3 | Selection of optimal wavelengths

Soft independent modeling of class analogy is a supervised classification method that applies data with recognized source defined as training samples to extract a classification pattern which can be used to classify new samples or test samples with undefined source in one of the groups. In SIMCA analysis, various classes are involved and distinct principal component models are made exclusively for each class. This means that each class has a PCA model. The new samples

are then evaluated within models and allocated to a group according to their similarity to the training samples (Mees et al., 2018). One of the results of SIMCA analysis is the discrimination power of the individual wavelength variables that can be used for optimal wavelength selection.

Soft independent modeling of class analogy analysis was accomplished with the statistical software of “The Unscrambler X” V10.4 (CAMO AS). The classification accuracy of healthy and infected samples was 60% in the 1st week after inoculation. The reason for obtaining low detection percentages is the small number of test samples, that is, 5 in each healthy and infected class, thus 3 of 5 healthy samples and 3 of 5 infected samples were correctly identified. However, the discrimination power plot of wavelength variables in the 1st week was demonstrated in Figure 8. Given that the discrimination power above 3 indicates that the variable is effective in separating the two classes, important wavelengths are selected. According to Figure 8, in the range of 400–700 nm, only the 507 nm had a discrimination power of more than 3, which was the effective wavelength in the visible range for identifying healthy from infected samples at the 1st week after inoculation. In the range of 700–1000 nm, most of the wavelengths were effective in classifying the two classes, but the discrimination power of the wavelengths of 713, 933, 937, and 950 nm was much higher. The wavelength range of 700–1100 nm is relevant to sugar and water content as it includes the second and third overtone of OH stretching and vibrations (Magwaza et al., 2012). The wavelength around 933 nm could be related to the third overtone of CH₂ vibration. The wavelength around 950 nm is also related to the O-H and C-H bonds. The 600–750 nm spectra were highly influenced by skin chlorophyll, which had an absorbance wavelength around 680 nm (Wang et al., 2015). Thus, the wavelength around 713 nm could be effective due to the skin chlorophyll.

The classification accuracy of healthy and infected samples in the 2nd week was 60 and 40%, respectively.

The reason for obtaining low detection percentages is the small number of test samples. However, Figure 9 illustrates the discrimination power plot of wavelength variables of the 2nd week. The discrimination power of the 522 and 787 nm wavelengths was higher than 3 and much higher than the other wavelengths, thus, they were selected as the effective wavelengths. The wavelength around 787 nm could occur because of third overtone of O-H and fourth overtone of C-H, and 522 nm was due to pigments absorbance (Jamshidi et al., 2012).

TABLE 4 Paired samples *t*-test to compare the spectral mean of healthy and infected orange samples in the 2nd week after inoculation

Spectral range	Groups	Descriptive statistics		Results		
		Number	Mean	<i>t</i>	<i>df</i>	Sig (two-tailed)
200–1100 nm	Healthy	1627	0.3421	102.261	1626	0.000
	Infected	1627	0.3205			
550–1050 nm	Healthy	900	0.0882	183.730	899	0.000
	Infected	900	0.0752			

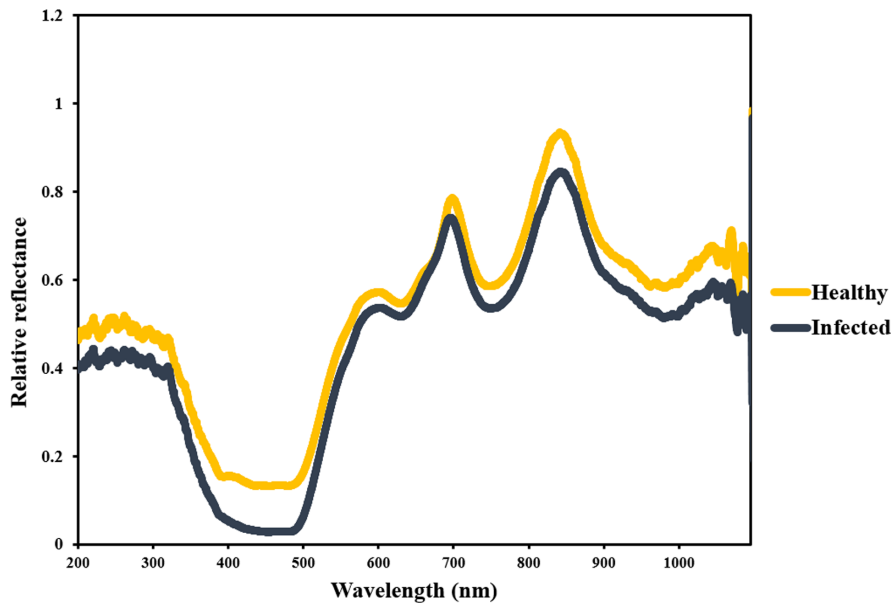


FIGURE 7 Average intractance spectra of healthy and infected samples in the 3rd week after inoculation

Spectral range	Groups	Descriptive statistics		Results		
		Number	Mean	t	df	Sig (two-tailed)
200–1100 nm	Healthy	1627	0.2049	116.837	1626	0.000
	Infected	1627	0.2170			

TABLE 5 Paired samples t-test to compare the spectral mean of healthy and infected orange samples in the 3rd week after inoculation

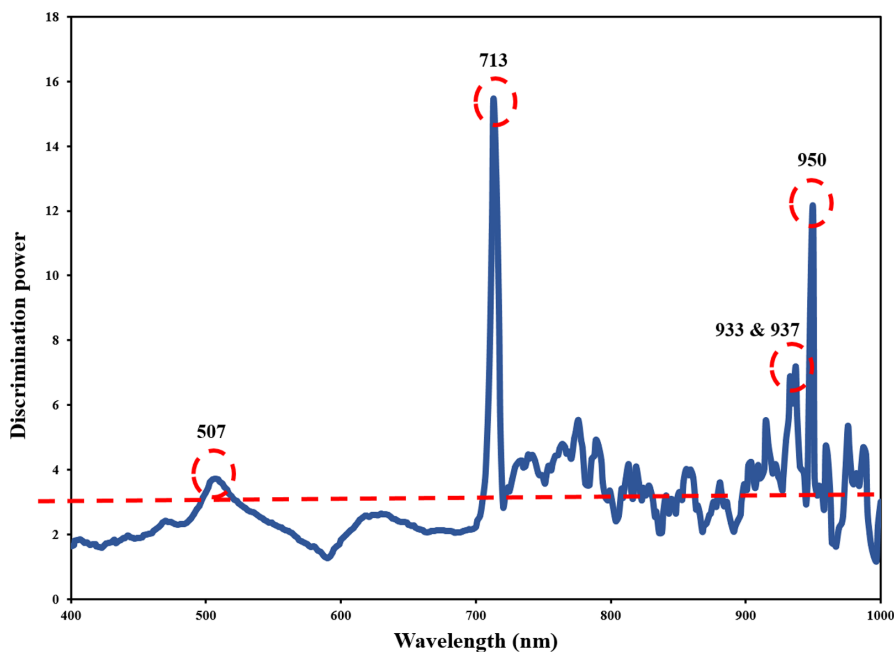


FIGURE 8 Discrimination power of different wavelengths in the separation of healthy from infected samples in the 1st week

The storage material that may be found in the fungal cell is glycogen or fat. Glycogen is especially evident in mature hyphae or reproductive organs (Gwynne-Vaughan & Barnes, 1937). The cell wall of fungi is also known as microfibrils of skeletal compounds such as β -glucan and chitin dispersed within the amorphous matrix. Beta-glucan and chitin are both polysaccharides. Most fungi have a chitin wall (Walker & White, 2011), and the mentioned compounds contain C-H bonds.

The classification accuracy of healthy and infected samples was 100% in the 3rd week after inoculation. Figure 10 illustrates the discrimination power plot of wavelength variables in the 3rd week. Most wavelengths were effective in classifying the two classes, but the discrimination power of the wavelengths of 546, 660, 691, and 839 nm was much higher. There were several peaks in the spectral range of 800–900 nm, including 805, 822, 832, 839, 862, 874, and 895 nm, indicating that the spectral range of

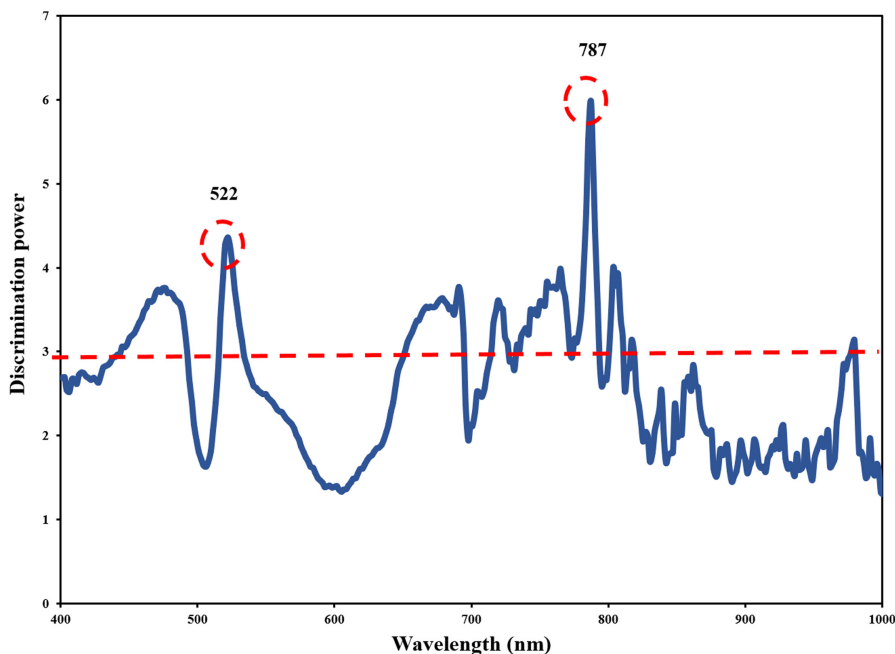


FIGURE 9 Discrimination power of different wavelengths in the separation of healthy from infected samples in the 2nd week

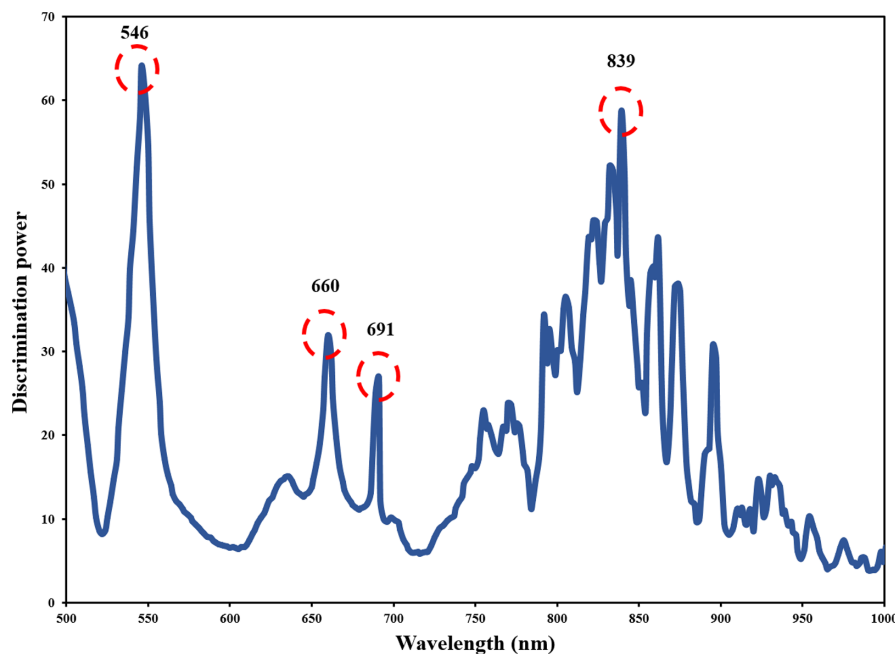


FIGURE 10 Discrimination power of different wavelengths in the separation of healthy from infected samples in the 3rd week

800–900 nm was very effective in detection of healthy and infected samples. The wavelength around 839 nm corresponds to the second overtone of O-H compounds (Magwaza et al., 2012). Wavelengths between 800 and 900 nm are related to CH, CH₂, and CH₃ bonds (Cen & He, 2007). The areas around 500 and 680 are related to anthocyanin and chlorophyll pigments absorbance (Khodabakhshian et al., 2017).

4 | CONCLUSION

The aim of this study was to investigate the spectral pattern of oranges infected with *A. alternata* and to determine the effective spectra in early detection of internal citrus black rot. In order to investigate whether the structure of the fungus affects the spectral pattern of the product, an experiment was first performed with infected orange juice

and healthy orange juice. First, the absorption value of solutions was obtained in the spectral range of 400–1100 nm at intervals of 100 nm. Then, the continuous spectrum of solutions was provided by another spectrophotometer in the spectral range of 200–700 nm.

Absorption values showed that adding *Alternaria* spores to orange juice had an effect on its absorption, and fungal-infected orange juice had a higher absorption amount than orange juice. Also, the absorption decreased with increasing wavelength. The infected orange juice resulted in a distinguished discrepancy in the spectra because of the peaks and shifts generated in continuous spectra. Spectral peaks of orange juice infected with *Alternaria* were 280, 335, 320, 360, and 420 nm. It can be said that adding fungus spores to orange juice had caused a peak shift from 280 nm to 320 nm and a peak shift from 320 nm to 360 nm and a significant increase in the absorption of these wavelengths occurred.

Jaffa oranges that were inoculated by *Alternaria alternata* in laboratory conditions were examined by a multichannel spectrometer in the range 200–1100 nm for 3 consecutive weeks after inoculation. After the extraction of relative spectra, soft independent modeling of class analogy was implemented on the spectra and classification of healthy samples from infected ones was done. The most important wavelengths for inspection of infection were achieved by a discrimination power plot of SIMCA analysis. The effective wavelengths in identifying healthy samples from infected ones in the 1st week were 507, 933, 937, and 950 nm with a classification accuracy of 60%. The effective wavelengths in classifying healthy samples from infected ones in the 2nd week were 522 and 787 nm with detection percentages of 60 and 40%, respectively. Also, wavelengths of 546, 660, 691, and 839 were found to be effective in classifying two groups with a classification accuracy of 100%.

ACKNOWLEDGMENTS

We, the authors, acknowledge Ferdowsi University of Mashhad for providing the funding for doing this research (Grant No. 3/48638). We would also acknowledge the Iran National Science Foundation (INSF) for providing the funding for doing this research (Grant No. 98000184).

CONFLICT OF INTEREST

The authors declare that they have no conflict of interest.


ETHICAL APPROVAL


This article does not contain any studies within human and animal subjects.

DATA AVAILABILITY STATEMENT

The data that support the findings of this study are not publicly available due to privacy or ethical restrictions.

ORCID

Narges Ghanei Ghooshkhaneh  <https://orcid.org/0000-0002-6176-5440>

Mahmood Reza Golzarian  <https://orcid.org/0000-0002-8370-1966>

REFERENCES

- Abad-Garcia, B., Berrueta, L. A., Garmon-Lobato, S., Gallo, B., & Vicente, F. (2009). A general analytical strategy for the characterization of phenolic compounds in fruit juices by high-performance liquid chromatography with diode array detection coupled to electrospray ionization and triple quadrupole mass spectrometry. *Journal of Chromatography A*, 1216(28), 5398–5415. <https://doi.org/10.1016/j.chroma.2009.05.039>
- Alander, J. T., Bochko, V., Martinkauppi, B., Saranwong, S., & Mantere, T. (2013). A review of optical nondestructive visual and near-infrared methods for food quality and safety. *International Journal of Spectroscopy*, 2013, 36. Article ID 341402. <https://doi.org/10.1155/2013/341402>
- Amodio, M. L., Ceglie, F., Chaudhry, M. M. A., Piazzolla, F., & Colelli, G. (2017). Potential of NIR spectroscopy for predicting internal quality and discriminating among strawberry fruits from different production systems. *Postharvest Biology and Technology*, 125, 112–121. <https://doi.org/10.1016/j.postharvbio.2016.11.013>
- Antonucci, F., Pallottino, F., Paglia, G., Palma, A., D'Aquino, S., & Menesatti, P. (2011). Non-destructive estimation of mandarin maturity status through portable VIS-NIR spectrophotometer. *Food and Bioprocess Technology*, 4(5), 809–813. <https://doi.org/10.1007/s11947-010-0414-5>
- Beć, K. B., & Huck, C. W. (2019). Breakthrough potential in near-infrared spectroscopy: Spectra simulation. A review of recent developments. *Frontiers in Chemistry*, 7, 48. <https://doi.org/10.3389/fchem.2019.00048>
- Bobelyn, E., Serban, A.-S., Nicu, M., Lammertyn, J., Nicolai, B. M., & Saey, W. (2010). Postharvest quality of apple predicted by NIR-spectroscopy: Study of the effect of biological variability on spectra and model performance. *Postharvest Biology and Technology*, 55(3), 133–143. <https://doi.org/10.1016/j.postharvbio.2009.09.006>
- Bock, J. E., & Connelly, R. K. (2008). Innovative uses of near-infrared spectroscopy in food processing. *Journal of Food Science*, 73(7), R91–R98. <https://doi.org/10.1111/j.1750-3841.2008.00870.x>
- Buyukcan, M. B., & Kavdir, I. (2017). Prediction of some internal quality parameters of apricot using FT-NIR spectroscopy. *Journal of Food Measurement and Characterization*, 11(2), 651–659. <https://doi.org/10.1007/s11694-016-9434-9>
- Carvalho, D. D. C., Alves, E., Batista, T. R. S., Camargos, R. B., & Lopes, E. A. G. L. (2008). Comparison of methodologies for conidia production by *Alternaria alternata* from citrus. *Brazilian Journal of Microbiology*, 39, 792–798. <https://doi.org/10.1590/S1517-8382008000400036>
- Cen, H., & He, Y. (2007). Theory and application of near infrared reflectance spectroscopy in determination of food quality. *Trends in Food Science & Technology*, 18(2), 72–83. <https://doi.org/10.1016/j.tifs.2006.09.003>
- Clark, C. J., McGlone, V. A., De Silva, H. N., Manning, M. A., Burdon, J., & Mowat, A. D. (2004). Prediction of storage disorders of kiwifruit (*Actinidia chinensis*) based on visible-NIR spectral characteristics at harvest. *Postharvest Biology and Technology*, 32(2), 147–158. <https://doi.org/10.1016/j.postharvbio.2003.11.004>
- Cohen, E., & Saguy, I. (1988). *Spectral Characteristics of Citrus Products*, in *Analysis of Nonalcoholic Beverages* (pp. 69–79). ed. By H.-F. Linskens, J. F. Jackson. Springer Berlin Heidelberg.
- El-Otmani, M., Ait-Oubahou, A., Zacarias, L. (2011). *Citrus spp.: orange, mandarin, tangerine, clementine, grapefruit, pomelo, lemon and lime*, in *Postharvest Biology and Technology of Tropical and Subtropical Fruits* (pp. 437–516). ed. By E. M. Yahia. Woodhead Publishing.
- Gabriel, M. F., Uriel, N., Teifoori, F., Postigo, I., Sunen, E., & Martinez, J. (2017). The major *Alternaria alternata* allergen, Alt 1: A reliable and specific marker of fungal contamination in citrus fruits. *International Journal of Food Microbiology*, 257, 26–30. <https://doi.org/10.1016/j.ijfoodmicro.2017.06.006>

- García-Sánchez, F., Galvez-Sola, L., Nicolás, J. J. M., Muelas-Domingo, R., & Nieves, M. (2017). *Using Near-Infrared Spectroscopy in Agricultural Systems, in Developments in Near-Infrared Spectroscopy*, ed. By K. G. Kyprianidis and J. Skvaril. IntechOpen.
- Goldschmidt, E. E., Goren, R., Monselise, S. P., Takahashi, N., Igoshi, H., Yamaguchi, I., & Hirose, K. (1971). Auxins in citrus: A reappraisal. *Science*, 174(4015), 1256–1257. <https://doi.org/10.1126/science.174.4015.1256>
- Guleria, S. P. S. (2000). *Quality assurance for fruits, vegetables and their products, in Postharvest technology of fruits and vegetables*, ed. By L.R. Verma, V.K. Joshi. Induce publishing Co..
- Gwynne-Vaughan, H. C. I., & Barnes, B. (1937). *The Structure and Development of the Fungi*. Cambridge University Press.
- Han, D., Tu, R., Lu, C., Liu, X., & Wen, Z. (2006). Nondestructive detection of brown core in the Chinese pear 'Yali' by transmission visible-NIR spectroscopy. *Food Control*, 17(8), 604–608. <https://doi.org/10.1016/j.foodcont.2005.03.006>
- Jamshidi, B., Minaei, S., Mohajerani, E., & Ghassemian, H. (2012). Reflectance Vis/NIR spectroscopy for nondestructive taste characterization of Valencia oranges. *Computers and Electronics in Agriculture*, 85, 64–69. <https://doi.org/10.1016/j.compag.2012.03.008>
- Jha, S. N., Narsaiah, K., Jaiswal, P., Bhardwaj, R., Gupta, M., Kumar, R., & Sharma, R. (2014). Nondestructive prediction of maturity of mango using near infrared spectroscopy. *Journal of Food Engineering*, 124, 152–157. <https://doi.org/10.1016/j.jfoodeng.2013.10.012>
- Jie, D., Zhou, W., & Wei, X. (2019). Nondestructive detection of maturity of watermelon by spectral characteristic using NIR diffuse transmittance technique. *Scientia Horticulturae*, 257, 108718. <https://doi.org/10.1016/j.scienta.2019.108718>
- Khodabakhshian, R., Emadi, B., Khojastehpour, M., Golzarian, M. R., & Sazgarnia, A. (2017). Development of a multispectral imaging system for online quality assessment of pomegranate fruit. *International Journal of Food Properties*, 20(1), 107–118. <https://doi.org/10.1080/10942912.2016.1144200>
- Kuroki, S., Nishino, M., Nakano, S., Deguchi, Y., & Itoh, H. (2017). Positioning in spectral measurement dominates estimation performance of internal rot in onion bulbs. *Postharvest Biology and Technology*, 128, 18–23. <https://doi.org/10.1016/j.postharvbio.2017.02.001>
- Magwaza, L. S., Opara, U. L., Nieuwoudt, H., Cronje, P. J. R., Saeys, W., & Nicolaï, B. (2012). NIR spectroscopy applications for internal and external quality analysis of citrus fruit—a review. *Food and Bioprocess Technology*, 5(2), 425–444. <https://doi.org/10.1007/s11947-011-0697-1>
- Magwaza, L. S., Opara, U. L., Terry, L. A., Landahl, S., Cronje, P. J. R., Nieuwoudt, H. H., Hanssens, A., Saeys, W., & Nicolaï, B. M. (2013). Evaluation of Fourier transform-NIR spectroscopy for integrated external and internal quality assessment of Valencia oranges. *Journal of Food Composition and Analysis*, 31(1), 144–154. <https://doi.org/10.1016/j.jfca.2013.05.007>
- Mees, C., Souard, F., Delporte, C., Deconinck, E., Stoffelen, P., Stéveny, C., Kauffmann, J.-M., & De Braekeleer, K. (2018). Identification of coffee leaves using FT-NIR spectroscopy and SIMCA. *Talanta*, 177, 4–11. <https://doi.org/10.1016/j.talanta.2017.09.056>
- Mishra, P., Woltering, E., Brouwer, B., & Hogeveen-van Echtelt, E. (2021). Improving moisture and soluble solids content prediction in pear fruit using near-infrared spectroscopy with variable selection and model updating approach. *Postharvest Biology and Technology*, 171, 111348. <https://doi.org/10.1016/j.postharvbio.2020.111348>
- Mogollon, M. R., Jara, A. F., Contreras, C., & Zoffoli, J. P. (2019). Quantitative and qualitative VIS-NIR models for early determination of internal browning in 'Cripps Pink' apples during cold storage. *Postharvest Biology and Technology*, 161, 111060. <https://doi.org/10.1016/j.postharvbio.2019.111060>
- Mojerlou, S. (2012). Phylogenetic analysis of *Alternaria* species associated with citrus black rot in Iran. *Journal of Plant Pathology & Microbiology*, 3(7), 1000144. <https://doi.org/10.4172/2157-7471.1000144>
- Moltó, E., Blasco, J., & Gómez-Sanchis, J. (2010). *Analysis of Hyperspectral Images of Citrus Fruits, in Hyperspectral Imaging for Food Quality Analysis and Control* (pp. 321–348). ed. By D.-W. Sun. Academic Press.
- Moscetti, R., Haff, R. P., Stella, E., Contini, M., Monarca, D., Cecchini, M., & Massantini, R. (2015). Feasibility of NIR spectroscopy to detect olive fruit infested by *Bactrocera oleae*. *Postharvest Biology and Technology*, 99, 58–62. <https://doi.org/10.1016/j.postharvbio.2014.07.015>
- Ncama, K., Tesfay, S. Z., Fawole, O. A., Opara, U. L., & Magwaza, L. S. (2018). Non-destructive prediction of 'Marsh' grapefruit susceptibility to postharvest rind pitting disorder using reflectance Vis/NIR spectroscopy. *Scientia Horticulturae*, 231, 265–271. <https://doi.org/10.1016/j.scienta.2017.12.028>
- Peever, T. L., Carpenter-Boggs, L., Timmer, L. W., Carris, L. M., & Bhatia, A. (2005). Citrus black rot is caused by phylogenetically distinct lineages of *Alternaria alternata*. *Phytopathology*, 95(5), 512–518. <https://doi.org/10.1094/phyto-95-0512>
- Peña, W. E. L., Massaguer, P. R. d., & Teixeira, L. Q. (2009). Microbial modeling of thermal resistance of *alicyclobacillus acidoterrestris* cra7152 spores in concentrated orange juice with nisin addition. *Brazilian Journal of Microbiology*, 40(3), 601–611. <https://doi.org/10.1590/S1517-83822009000300024>
- Pissard, A., Fernandez Pierna, J. A., Baeten, V., Sinnaeve, G., Lognay, G., Mouteau, A., Dupont, P., Rondia, A., & Lateur, M. (2013). Non-destructive measurement of vitamin C, total polyphenol and sugar content in apples using near-infrared spectroscopy. *Journal of the Science of Food and Agriculture*, 93(2), 238–244. <https://doi.org/10.1002/jsfa.5779>
- Pombeiro-Sponchiado, S. R., Sousa, G. S., Andrade, J. C. R., Lisboa, H. F., & Gonçalves, R. C. R. (2017). *Production of Melanin Pigment by Fungi and Its Biotechnological Applications, in Melanin*. ed. By M. Blumenberg. IntechOpen.
- Qing, Z., Ji, B., & Zude-Sasse, M. (2007). Wavelength selection for predicting physicochemical properties of apple fruit based on near-infrared spectroscopy. *Journal of Food Quality*, 30, 511–526. <https://doi.org/10.1111/j.1745-4557.2007.00139.x>
- Riza, D. F. A., Suzuki, T., Ogawa, Y., & Kondo, N. (2017). Diffuse reflectance characteristic of potato surface for external defects discrimination. *Postharvest Biology and Technology*, 133, 12–19. <https://doi.org/10.1016/j.postharvbio.2017.07.006>
- Sánchez, M. T., Torres, I., Gil, B., Pérez-Marín, D., Garrido-Varo, A., & De la Haba, M. J. (2018). In-situ determination of external quality parameters in intact summer squash using near-infrared reflectance spectroscopy. *Acta Horticulture*, 1194, 1259–1264. <https://doi.org/10.17660/ActaHortic.2018.1194.178>
- Sun, H., Wang, L., Zhang, B., Ma, J., Hettenhausen, C., Cao, G., Sun, G., Wu, J., & Wu, J. (2014). Scopoletin is a phytoalexin against *Alternaria alternata* in wild tobacco dependent on jasmonate signaling. *Journal of Experimental Botany*, 65(15), 4305–4315. <https://doi.org/10.1093/jxb/eru203>
- Teerachaichayut, S., Kil, K. Y., Terdwongworakul, A., Thanapase, W., & Nakanishi, Y. (2007). Non-destructive prediction of translucent flesh disorder in intact mangosteen by short wavelength near infrared spectroscopy. *Postharvest Biology and Technology*, 43(2), 202–206. <https://doi.org/10.1016/j.postharvbio.2006.09.007>
- Teerachaichayut, S., Terdwongworakul, A., Thanapase, W., & Kiji, K. (2011). Non-destructive prediction of hardening pericarp disorder in intact mangosteen by near infrared transmittance spectroscopy. *Journal of Food Engineering*, 106(3), 206–211. <https://doi.org/10.1016/j.jfoodeng.2011.05.007>

- Thomma, B. P. (2003). *Alternaria* spp.: From general saprophyte to specific parasite. *Molecular Plant Pathology*, 4(4), 225–236. <https://doi.org/10.1046/j.1364-3703.2003.00173.x>
- Timmer, L. W., Garnsey, S. M., & Broadbent, P. (2003). *Diseases of citrus*, in *Diseases of tropical fruit crops*. ed. By R.C. Ploetz, CAB International.
- Timmer, L. W., Peever, T. L., Solel, Z., & Akimitsu, K. (2003). *Alternaria* diseases of citrus—novel pathosystems. *Phytopathologia Mediterranea*, 42(2), 99–112. https://doi.org/10.14601/Phytopathol_Mediterr-1710
- Toledo-Martín, E. M., García-García, M. C., Font, R., Moreno-Rojas, J. M., Gómez, P., Salinas-Navarro, M., & Del Río-Celestino, M. (2015). Application of visible/near-infrared reflectance spectroscopy for predicting internal and external quality in pepper. *Journal of the Science of Food and Agriculture*, 96(9), 3114–3125. <https://doi.org/10.1002/jsfa.7488>
- Troncoso-Rojas, R., & Tiznado-Hernández, M. E. (2014). *Alternaria alternata* (black rot, black spot), in *Postharvest decay* (pp. 147–187), ed. By S. Bautista-Baños. Academic Press.
- Uwadaira, Y., Sekiyama, Y., & Ikehata, A. (2018). An examination of the principle of non-destructive flesh firmness measurement of peach fruit by using VIS-NIR spectroscopy. *Heliyon*, 4(2), e00531. <https://doi.org/10.1016/j.heliyon.2018.e00531>
- Walker, G. M., & White, N. A. (2011). *Introduction to fungal physiology*, in *Fungi: Biology and Applications* (pp. 1–34), ed. By K. Kavanagh, John Wiley & Sons, Inc.
- Wang, H., Peng, J., Xie, C., Bao, Y., & He, Y. (2015). Fruit quality evaluation using spectroscopy technology: A review. *Sensors (Basel)*, 15(5), 11889–11927. <https://doi.org/10.3390/s150511889>
- Zude, M. (2009). *Optical monitoring of fresh and processed agricultural crops*. CRC.

How to cite this article: Ghanei Ghooshkhaneh, N., Golzarian, M. R., & Mamarabadi, M. (2022). Spectral pattern study of citrus black rot caused by *Alternaria alternata* and selecting optimal wavelengths for decay detection. *Food Science & Nutrition*, 10, 1694–1706. <https://doi.org/10.1002/fsn3.2739>